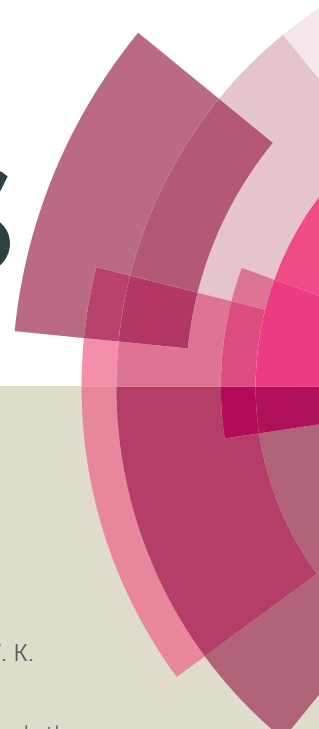


RSC Advances



This article can be cited before page numbers have been issued, to do this please use: U. J. Chaube, V. K. Vyas and H. G. BHATT, *RSC Adv.*, 2016, DOI: 10.1039/C5RA27017K.



This is an *Accepted Manuscript*, which has been through the Royal Society of Chemistry peer review process and has been accepted for publication.

Accepted Manuscripts are published online shortly after acceptance, before technical editing, formatting and proof reading. Using this free service, authors can make their results available to the community, in citable form, before we publish the edited article. This *Accepted Manuscript* will be replaced by the edited, formatted and paginated article as soon as this is available.

You can find more information about *Accepted Manuscripts* in the [Information for Authors](#).

Please note that technical editing may introduce minor changes to the text and/or graphics, which may alter content. The journal's standard [Terms & Conditions](#) and the [Ethical guidelines](#) still apply. In no event shall the Royal Society of Chemistry be held responsible for any errors or omissions in this *Accepted Manuscript* or any consequences arising from the use of any information it contains.

Design and Synthesis of Potent *N*-Phenylpyrimidine Derivatives for the Treatment of Skin Cancer

Udit J. Chaube, Vivek K. Vyas, Hardik G. Bhatt*

Department of Pharmaceutical Chemistry, Institute of Pharmacy, Nirma University, Ahmedabad 382 481. India.

**Corresponding author Information:*

Department of Pharmaceutical Chemistry, Institute of Pharmacy, Nirma University, S. G. Highway, Chharodi, Ahmedabad 382 481. India

Tel.: +91 79 30642727; Fax: +91 2717 241916; E-mail: hardikbhatt23@hotmail.com

Abstract

Development of novel synthetic compounds for the treatment of skin cancer is much needed, as there are sudden rise in incidences of skin cancer throughout the world and available chemotherapy is facing problems of resistance. Hence, present research efforts were made to discover potent molecules against skin cancer. Pharmacophore models were developed by using GALAHAD module of Sybyl X followed by validation, virtual screening, design and *in silico* ADMET studies. Based on features generated in computational studies and structural importance of pyrimidine moiety in highest Q_{FIT} value molecule of virtual hit; it was selected as a core moiety for further designing of molecules. Fourteen substituted pyrimidine derivatives were designed, synthesized and characterised by 1H and ^{13}C NMR, mass and elemental analysis, while purity was checked by HPLC. All these compounds were evaluated for *in vitro* studies on five cancer lines; from which, compounds **6a**, **6h**, **6j** and **6k** were found potent, specifically on skin cancer cell line. Based upon results of *in vitro* studies, they were selected further, along with 5-FU, for *in vivo* study by DMBA induced skin cancer model. Compound **6h** showed favourable actions against skin cancer and treated tumours demonstrating potential of the series. This study could be explored in future to design lead molecule for the treatment of skin cancer.

Keywords: Skin cancer, Pharmacophore modelling, Virtual screening, *N*-Phenylpyrimidine, X-ray crystallography.

1. Introduction

Cancer is a disease with uncontrolled proliferation of cells and the potential with which it can invade to any part of the body. Cancer is one of the leading cause of death in the world and the second most common disease after cardiovascular disorders.¹ It is predicted that by the end of the year 2020, approximately 16.5 million new cases will be detected, and most of them from the developing countries.¹ Various preventive measures are now available for the treatment of cancers, but few cancers such as skin cancer have no preventive measures. Rendering to world cancer report of WHO, skin cancer constitutes nearly 30% of all recently diagnosed cancers in the world.¹⁻³ Difficulty associated in the treatment of skin cancer is the resistance to existing chemotherapy due to the presence of survivin molecule in the cell.² Few cytotoxic drugs are available for the treatment of skin cancer, however, they exhibit toxic effects on kidney, lung, heart, brain, and gastrointestinal tract.⁴ If skin cancer cannot be diagnosed at early stage, then it can metastasized to various parts of the body through the lymph system and blood circulation. UV radiations are mainly responsible for the development of skin cancer^{5,6} through the direct and indirect mechanisms like immune suppression, formation of cyclobutane pyrimidine dimers, p53 gene mutation, oxidative stress, etc.⁷⁻⁹ Another factor, which is responsible for the skin cancer, is fair complexion due to deficiency of UV-blocking pigment known as eumelanin.⁹ Ozone layer depletion, altitude, latitude and weather conditions also affect the intensity of UV radiations. Rudimentary mechanism behind the pathogenesis of skin cancer due to UV radiation is the dented DNA, which results in the formation of assembly of bad cell^{4,8} and the end result of this is the formation of tumour. Normally, p53 protein triggers p21 protein and this intrudes the cell cycle in between G1 and S phase. Due to the mutation in the p53 protein, this normal process get disturbed, which upshots into the copious growth of defective cells resulted into the skin cancer. Hence, development of novel chemical compounds for the treatment of skin cancer is

desirable goal of this work. Here, efforts were made to design novel pyrimidine derivatives via pharmacophore-based scaffold hopping method. Designed molecules were synthesised and evaluated against different cancer cell lines including skin cancer cell line (A-375). Potent compounds in *in vitro* evaluation were further evaluated for *in vivo* evaluation by DMBA induced skin cancer animal model.

2. Results and Discussion

2.1 Rational for design of compounds

Involvement of CDK2 in skin cancer via p53 and p21 protein is well known, hence in this work, eight molecules (**1-8**), (Table ST-1 under supplementary information) were taken from the published literature¹⁰⁻¹⁵ for the generation of pharmacophore models. Twenty pharmacophore models were generated through the GALAHAD module of Sybyl X,¹⁶ among them, model-15 (Table ST-2 under supplementary information) was selected as best model based on lowest energy value, maximum number of hits, and comparatively higher specificity value.¹⁷⁻²⁰ 2D representation of the best model 15 is shown in Figure 1 (3D-representation is shown as Figure SF-1 under supplementary information), which consisted of 2 donor atoms, 2 hydrophobic sites, and 1 acceptor atom. Validation of best pharmacophore model was carried out by GH (Guner Henry) scoring method and ROC (Receiver Operating Characteristics) curve analysis to check the accuracy and reliability of model.²¹⁻²³ GH score and area under curve (AUC) of ROC curve analysis of model-15 was 0.703 and 0.7, respectively (Table ST-3 and ST-4 under supplementary information). Pharmacophore model-15 was used as a 3D search query against NCI database, which consisted of 250000 diverse anticancer molecules. Compounds having various chemical groups spatially overlap (map) with corresponding features of pharmacophoric model 15 and were captured as hits with Q_{FIT} value. Retrieved hit NCIIDM81922 with highest Q_{FIT} value of 93.18 consisted of pyrimidine

ring as core moiety in the structure. (Structures of top five hit molecules and their Q_{FIT} values are given in supplementary information).

N-Phenylpyrimidine was selected as a core moiety for the design of compounds based on maximum similarity with the generated pharmacophore. Another advantage associated with the selection of *N*-phenylpyrimidine ring is the presence of pyrimidine ring, which is similar to the most effective marketed drug, 5-fluorouracil (5-FU), available for the treatment of skin cancer. Based upon these facts and results of pharmacophore modelling, fourteen novel derivatives were designed and synthesized (**6a-n**) (**Scheme 1**). In the designed series, different substitutions were carried out at R_1 (**C-5**) and R_2 (**C-4**) positions of *N*-phenylpyrimidine ring. Two different series were prepared by using two different starting materials; methylcyanoacetate and ethylcyanoacetate, which resulted into methyl and ethyl substitution at R_1 position of *N*-phenylpyrimidine moiety. Different aliphatic and aromatic amines were substituted at R_2 position to check the effect of additional hydrophobic group on the skin cancer activity. The designed compounds were predicted for *in silico* toxicity risk prediction parameters. Factors of toxicity risk management are mutagenicity, tumorigenicity, irritant effect and reproductive effect. Results of toxicity prediction study revealed that four compounds viz. **6f**, **6g**, **6m**, and **6n** are at risk of mutagenic toxicity; compounds **6g** and **6n** showed tumorigenic effect; compounds **6f** and **6m** showed irritant effect. All other compounds are non-toxic. (Table ST-5 under supplementary information).

3. Chemistry

Our previously reported synthetic scheme²⁴ was utilised as a reference for the synthesis of intermediates and for the target compounds. As shown in scheme 1, methyl or ethyl substituted S,S-acetal (**2a,b**) was afforded from methylcyanoacetate or ethylcyanoacetate,

respectively, by reacting with carbon disulphide in the presence of base, potassium hydroxide (step-I). Step-II involved nucleophilic displacement of one -SCH₃ group from S,S-acetal (**2a,b**) by aniline which resulted in the formation of methyl or ethyl substituted S,N-acetal (**3a,b**). Step-II product (**3a,b**) was treated with formamidine acetate in presence of sodium hydroxide and ethanol to afford product (**4a,b**), which got cyclised to give pyrimidine moiety (**5a,b**) in the presence of HCl saturated dioxane. HCl is known to enhance the reactivity of -CN group, which resulted into formation of 5-substituted-6-(*N*-phenyl)-4-chloropyrimidine (**5a,b**) as a core moiety. This core moiety was utilised for the synthesis of designed compounds as shown in synthetic Scheme 1. Chlorine on pyrimidine ring was a point for nucleophilic substitution by different amines. Seven different aliphatic as well as aromatic amines were substituted on pyrimidine moiety to afford 14 different final compounds (**6a-n**).

Chemical structure of all compounds were confirmed by ¹H and ¹³C NMR, mass spectral and elemental analysis data. Purity of compounds were determined from HPLC analysis (Table ST-6 under supplementary information). The significant features of ¹H NMR spectra include appearance of different sets of hydrogen atom resonances corresponding to the protons in the aromatic rings (on **C-4** and **C-6** of pyrimidine; aromatic protons on **C-6** phenyl ring are indicated by symbol- '), pyrimidine ring (at **C-2**), secondary amines (on **C-4** and **C-6** of pyrimidine), methyl and ethyl groups (as R₁). For synthesized compounds, set of protons corresponding to the aromatic ring appear in the range of 6.50-8.00 δ ppm, showing the expected multiplicity and integration values. The resonance peaks, in the region from 8.01-8.70 δ ppm, corresponds to the pyrimidine proton. These Ar-H of ¹H NMR spectrum are correlated with C atoms from 110-170 δ ppm in ¹³C NMR spectra. Signals for the secondary amine proton (-NH-) appear as singlet in the region of 8-11 δ ppm. For -CH₃ group of methyl acetate, singlet appears from 3.00 to 3.90 δ ppm. For -CH₃ of ethyl acetate, triplet appears in

the region of 1.20-1.40 δ ppm and for $-\text{CH}_2$ group of ethyl acetate, quartet appears in the region of 4.13-4.94 δ ppm (^1H NMR, ^{13}C NMR and Mass spectra of few representative compounds are provided in supplementary information). Crystal structure of compound **6h** was derived by single crystal X-ray analysis and is shown in Figure 2 (Detailed description of results of X-ray crystallography studies is provided in supplementary information. Crystal structure is deposited at the Cambridge Crystallographic Data Centre with deposition number CCDC 1438291).

4. Biological Evaluation

4.1 Antiproliferative *in vitro* assay

Synthesized derivatives were screened against five different cancer cell lines, viz. A-375, MCF-7, DU-145, HEP-3B and non-cancerous cell line VERO, and their IC_{50} values are reported in **Table 1**. Few compounds showed potent activity on various cell lines. Compounds **6a** ($\text{IC}_{50} = 0.0073\mu\text{M}$), **6h** ($\text{IC}_{50} = 0.0047\mu\text{M}$), **6j** ($\text{IC}_{50} = 0.0079\mu\text{M}$) and **6k** ($\text{IC}_{50} = 0.0876\mu\text{M}$) showed potent activity on skin (melanoma) cancer cell line, A-375. Compounds **6h** ($\text{IC}_{50} = 0.0075\mu\text{M}$), **6j** ($\text{IC}_{50} = 0.0042\mu\text{M}$) and **6n** ($\text{IC}_{50} = 0.016\mu\text{M}$) showed potent activity on breast cancer cell line MCF-7. Compounds **6h** ($\text{IC}_{50} = 0.0222\mu\text{M}$), **6k** ($\text{IC}_{50} = 0.0561\mu\text{M}$), **6l** ($\text{IC}_{50} = 0.018\mu\text{M}$) and **6m** ($\text{IC}_{50} = 0.0302\mu\text{M}$) showed potent activity on Hepatoma cancer cell line HEP-3B. Compounds **6b** ($\text{IC}_{50} = 0.0073\mu\text{M}$) and **6h** ($\text{IC}_{50} = 0.0075\mu\text{M}$) showed potent activity on Prostate cancer cell line DU-145. In case of VERO cell line, compounds **6c**, **6d**, **6e**, **6i** and **6l** were found cytotoxic on normal VERO cell line and rest of the compounds were found to be non-toxic, showing IC_{50} value $>500\mu\text{M}$. 5-FU showed IC_{50} values of $0.0042\mu\text{M}$ (on A-375), $1.60\mu\text{M}$ (on MCF-7), $1.75\mu\text{M}$ (on HEP-3B) and $0.07\mu\text{M}$ (on DU-145). From the results of *in vitro* activity of synthesized compounds, it was found that synthesized compounds showed most prominent activity on skin cancer cell

line (A-375). Hence, highest active compounds, **6a**, **6h**, **6j** and **6k**, were further selected for *in vivo* evaluation in swiss-albino mice by DMBA induced skin cancer model.

4.2 *In vivo* assay

In vivo study was carried out in Swiss-albino mice by 16 weeks DMBA induced skin cancer model. Serum biomarkers and oxidative stress parameter levels were checked 12 weeks after the induction of skin cancer in disease induced mice. A significant increase ($p < 0.05$) in the serum level of biomarkers viz. Gamma Glutamyl Transferase (GGT), Lactate Dehydrogenase (LDH), C-Reactive Protein (CRP); oxidative stress parameter, Malondialdehyde (MDA) and significant decrease in serum levels of other oxidative stress parameters viz. Reduced Glutathione (GSH) and Superoxide Dismutase (SOD) were observed in skin cancer induced mice as compared to normal control mice group, which confirmed the presence of skin cancer. After the treatment with synthesized compounds (2%) and standard 5-fluorouracil (5-FU) (2%) from 12th to 16th weeks, it was found that compound **6h** and 5-FU significantly reduced ($p < 0.05$) levels of GGT, LDH, CRP (Figures 3A, 3B and 3C) and MDA (Figure 4A); while, increased levels of GSH and SOD (Figures 4B, 4C) at the end of 16th week which demonstrated good anticancer activity. Statistical results of serum biomarkers and oxidative stress parameter levels are shown in **Table 2** and **3**, respectively. Tumour volume, tumour burden and survival rate were observed from 6th to 16th weeks after the induction of skin cancer and data are shown in **Table 4**. A significant increase ($p < 0.05$) in tumour volume and tumour burden were observed at the end of 12th week in disease (skin cancer) induced mice group. Effect of 5-FU and synthesized compounds **6a**, **6h**, **6j** and **6k** on tumour volume and tumour burden was observed from 12th to 16th week and it was found that at the end of 16th week, highest reduction in tumour volume and tumour burden was noted in the compound **6h** and 5-FU (Figures 5A and 5B). At the end of the study (16th week), no significant difference of serum biomarkers levels, oxidative stress parameters, tumour volume and tumour burden

was observed between compound **6h** and 5-FU treated groups, which confirmed the anticancer activity of **6h**. 100% survival rate was observed in the normal control group, skin cancer control group treated with 5-FU, **6h** and **6j** from 6th to 16th week.

Figure 7(A to D) represented photographs of caudal region skin of the mice and histopathological results of skin samples of normal control group, skin cancer control group, skin cancer treated with 5-FU and skin cancer treated with compound **6h**, respectively. Figure 7A, normal control group, represented normal caudal region skin of the mice and histopathological section having various layers of skin. In skin cancer control mice, photograph (Fig 7B) showed that generated tumour mass is thoroughly spread over the caudal region skin of the mice. Histopathological study also showed disruption of fatty layer with presence of keratin pearls. The presence of rete ridges extending through the connective tissue was also seen, along with the mark presence of dysplastic and hyperplastic epithelial cells. Photographs shown in Figure 7C and 7D showed that tumour mass was completely removed from the caudal region skin of the mice which were treated with compound **6h** and 5-FU. Histopathological sections of skin from mice treated with compound **6h** and 5-FU showed the complete absence of keratin pearls, dysplastic epithelial cells and rete ridges, which proved the potency of the **6h** for the treatment. (Colour representation is given as Figure SF-2)

5. Structure Activity Relationship

Structure activity relationship study of synthesized compounds for their effectiveness on all four cell lines, viz. Skin cancer, Breast cancer, Hepatoma cancer and Prostate cancer is discussed in this section.

R₁ substitution of the pyrimidine ring was substituted with methyl as well as ethyl groups to check the effect of bulkiness on the activity against the skin cancer cell line. Compounds with methyl substitution at R₁ position resulted into the lower activity as compared to ethyl substituted compounds, which clearly indicated that groups with higher carbon number like ethyl or higher at R₁ position is required to increase the potency of synthesized compounds. Apart from highest active compound **6h**, compounds with ethyl substitution at R₁ position (**6j**, **6k**, **6l** and **6n**) were found more potent than compounds **6c**, **6d**, **6e** and **6g**, which were substituted with methyl group at R₁ position. R₂ position on pyrimidine ring was substituted with aliphatic and aromatic amines. Results of *in vitro* anticancer activity revealed that compounds with aromatic amine exhibited more potent anticancer activity as compared to aliphatic amines. In the first series, compounds **6a**, **6b**, **6c** and **6d** exhibited more potent activity than compounds **6f** and **6g**; while in the second series, compounds **6h**, **6j**, **6k** and **6l** exhibited more potent activity than compounds **6m** and **6n**. The compounds which showed good *in vitro* anticancer activity were evaluated for *in vivo* anticancer assay. Four best compounds **6a**, **6h**, **6j** and **6k** were further screened for *in vivo* anticancer activity. Amongst them, compound **6h** showed most promising activity as compared to **6a**, **6j** and **6k** and emerged as the most potent compound of the series. Structural features like presence of ethyl group at R₁ position and sulphanilamide at R₂ position in compound **6h** are found crucial and required for anticancer activity.

In MCF-7 cell line, compounds **6h**, **6j** and **6k** were found more potent as compared to compounds **6a**, **6c** and **6d** proving the importance of ethyl substitution at R₁ position. Further, comparison between **6h**, **6j** and **6k** revealed that **6h** and **6j** were found more potent than compound **6k**, as compound **6k** consisted of electron withdrawing nitro group on aromatic amine at R₂ position, while compounds **6h** and **6j** consisted of the -SO₂NH₂ and -OCH₃, which are electron donating groups.

In HEP-3B cell line, compounds **6h**, **6i** and **6m** were found more potent as compared to **6a**, **6b** and **6e**. This result again proved the importance of the ethyl group at R₁ substitution which is present in case of **6h**, **6i** and **6m**. Further comparison between **6h**, **6i** and **6m** indicated that substitution at R₂ with substituted aromatic amine, specifically sulphanilamide, is more favourable in context with potency as compared to the alicyclic or aliphatic amine. This can be proved by the compounds **6h**, **6i** and **6m**, where **6i** and **6m** were found to be less potent as compared to the compound **6h**, which consisted of the aromatic amine like sulphanilamide at R₂ position, while in contrast, compound **6i** consisted of piperazine and compound **6m** consisted of urea at R₂ position.

On the other hand, methyl substitution at R₁ position was proved to be active against DU-145 cell line. This results were in contrast with other three cell line study results, where ethyl group at R₁ position was found more effective. This could be proved by compounds **6b** and **6d**, where compounds **6b** and **6d** were found more potent as compared to **6i** and **6k**. Further comparison between compounds **6b** and **6d** showed that compound **6b** was found more potent as compared to compound **6d**; as compound **6b** consisted of piperazine at R₂ substitution, while in case of compound **6d**, electron withdrawing group nitro group was present on aromatic amine at R₂ position.

6. Conclusion

Based upon the pharmacophore-based virtual screening fourteen novel *N*-Phenyl pyrimidine derivatives were designed, synthesised and evaluated against different cancer lines viz. skin cancer (A-375), breast cancer (MCF-7), hepatocellular carcinoma (HEP-3B) and prostate cancer (DU-14). Structure activity relationship study proved that ethyl group at R₁ and aromatic amines at R₂ positions of *N*-Phenyl pyrimidine were required for activity against the skin cancer (A-375). Similarly in case of breast cancer (MCF-7) ethyl group was proved

effective at R₁ position with electron donating substituted aromatic amine at R₂ position. In case of hepatocellular carcinoma (HEP-3B), R₂ position was found to be favourable for aromatic amines compared to alicyclic or aliphatic amines in combination with ethyl group at R₁ position. In contrast, methyl substitution at R₁ position was found more effective against prostate cancer (DU-145) in combination with electron donor amines at R₂ position. As compounds **6a**, **6h**, **6j** and **6k** revealed good anticancer activity against the skin cancer cell line (A-375), they were further evaluated in DMBA induced skin cancer animal model. Among these four derivatives, compound **6h** was found to be best as it treated the tumours completely. Results of biological screening were quite promising which indicated that compound **6h** is equipotent to 5-FU and it is considered as a good lead compound in future derivatization with bulky group at R₁ and aromatic amines at R₂ positions of *N*-Phenyl pyrimidine to design novel compound which can give good anticancer activity against the skin cancer.

7. Experimental Section

All reactions were performed using oven dried *borosilicate* glassware and dry solvents. Precoated silica gel plates (MERCK) were used for TLC to monitor progress of the reaction. UV chamber and iodine fume chamber were used for detection of spots on TLC plates. REMI Rota-mantle was used for refluxing and stirring the reactions. Rotary vacuum evaporator (BUCHI type) was used for the recovery of the solvents. IR lamp was used for drying products. Melting point was recorded on VEEGO corporation melting point apparatus. All the compounds were purified by column chromatography and purity of all the compounds were checked through the JASCO HPLC instrument. Purity of all the compounds was found to be more than 95%. Mass spectra were recorded on WATERS mass spectrometer using Electron Spray Ionization (ESI) as ion source. The ¹H and ¹³C NMR were recorded using

tetramethylsilane (TMS) as an internal standard on BRUKER AVANCE-II 400 MHz spectrometer. Chemical shifts (δ) were reported in ppm, downfield of TMS and coupling constants (J) are given in Hz. Single crystal XRD of most potent compound **6h** was recorded using RIGAKU SCX mini diffractometer.

Following procedures were used for synthesis of products **2a** to **5a**:

7.1 Synthesis of methyl-2-cyano-3,3-bis(methylthio)acrylate (2a): Potassium hydroxide (11.2g, 0.2mol) was weighed and dissolved in 5mL of water, 15mL of DMF was added with cooling and stirring was continued for 10min. In the stirring mixture, methylcyanoacetate (**1a**) (8.8mL, 0.1mol) was added, followed by carbon disulphide (6mL, 0.1mol). Above mixture was stirred for 1hr at 25°C and was cooled. DMS (18.9mL, 0.2mol) was added drop wise, maintaining the temperature at 0°C. Above mixture was added to the crushed ice. Yellow crystalline product of methyl-2-cyano-3,3-bis(methylthio)acrylate (**2a**) was precipitated out, washed with water and dried. The product was recrystallized with n-hexane yielding pure white colour needle shaped crystals (yield 65.88%, m.p. 54-56°C).

7.2 Synthesis of methyl-2-cyano-3-(methylthio)-3-(phenylamino)acrylate (3a): Compound **2a** (4.06g, 0.02mol) and aniline (1.82mL, 0.02mol) were refluxed in ethyl alcohol for 2hr. Resulted reaction mixture was cooled on the ice bath. White colour needle shaped crystals of methyl-2-cyano-3-(methylthio)-3-(phenylamino)acrylate (**3a**) were obtained, filtered and dried (yield 76.19%, m.p. 62-63°C).

7.3 Synthesis of methyl-3-(aminomethyleneamino)-2-cyano-3-(phenylamino)acrylate (4a): Formamidine acetate (2.08g, 0.02mol) was added to 1M ethanolic sodium hydroxide solution. Reaction mixture was allowed to stir for 45min. Compound **3a** (2.5g, 0.01mol) in ethanol was added drop wise by dropping funnel to the reaction mixture. The reaction

mixture was stirred for 6hr by maintaining the ice-cold condition and added to the crushed ice. White colour solid product of methyl-3-(aminomethyleneamino)-2-cyano-3-(phenylamino)acrylate (**4a**) was precipitated out, filtered and dried (yield 75.62 %, m.p. 69-71°C)

7.4 Synthesis of methyl-4-chloro-6-(phenylamino)pyrimidine-5-carboxylate (**5a**):

Compound **4a** (4.8g, 0.02mol) was added, with stirring, to 25mL of saturated solution of 1,4-dioxane with dry HCl gas. The stream of dry HCl gas was passed to the same reaction mixture for 24hr. Reaction mixture was added to the crushed ice. White precipitates were obtained and were filtered. Obtained compound methyl-4-chloro-6-(phenylamino)pyrimidine-5-carboxylate (**5a**) was again dissolved in the saturated bicarbonate solution to neutralize the excessive acid. The compound was filtered and dried (yield 66.37%, m.p. 57-59°C).

Following procedures were used for synthesis of products **2b** to **5b**:

7.5 Synthesis of ethyl-2-cyano-3,3-bis(methylthio)acrylate (2b**):** Same as compound **2a**; instead of methylcyanoacetate, ethylcyanoacetate (**1b**) (10.6mL, 0.1mol) was used and resulted into yellow crystalline product **2b**. The product was recrystallized from n-hexane yielded pure white colour needle shaped crystals (yield 63.14%, m.p. 56-58°C).

7.6 Synthesis of ethyl-2-cyano-3-(methylthio)-3-(phenylamino)acrylate (3b**):** Same as compound **3a**; instead of methyl-2-cyano-3,3-bis(methylthio)acrylate, ethyl-2-cyano-3,3-bis(methylthio)acrylate (**2b**) (2.17g, 0.01mol) was used and resulted into white colour needle shaped crystalline product **3b** (yield 51.52%, m.p. 65-67°C).

7.7 Synthesis of ethyl-3-(-aminomethyleneamino)-2-cyano-3-(phenylamino)acrylate (4b): Same as compound **4a**; instead of methyl-2-cyano-3-(methylthio)-3-(phenylamino)acrylate, ethyl-2-cyano-3-(methylthio)-3-(phenylamino)acrylate (**3b**) (2.6g, 0.01mol) was used and resulted into white colour solid product **4b** (yield 76.92%, m.p. 70-73°C).

7.8 Synthesis of ethyl-4-chloro-6-(phenylamino)pyrimidine-5-carboxylate (5b): Same as compound **5a**; instead of methyl-3-(-aminomethyleneamino)-2-cyano-3-(phenylamino)acrylate, ethyl-3-(-aminomethyleneamino)-2-cyano-3-(phenylamino)acrylate (**4b**) (5.16g, 0.02mol) was used which resulted into white colour solid product **5b** (yield 63.29%, m.p. 90-92°C).

Following procedures were used for synthesis of final step products **6a** to **6n**:

7.9 Synthesis of methyl-4-benzenesulfonamide-6-(phenylamino)pyrimidine-5-carboxylate (6a). Methyl-4-chloro-6-(phenylamino)pyrimidine-5-carboxylate (**5a**) (2.6g, 0.01mol) was mixed with the sulphanilamide (1.7g, 0.01mol) in 15mL of isopropyl alcohol. Catalytic amount of the concentrated HCl was added to the reaction mixture and was refluxed for 6hr and transferred to the crushed ice. White solids of **6a** got precipitated out, filtered and dried (yield 55%, m.p. 210-212°C). ¹H NMR (400 MHz, DMSO-*d*₆) δ PPM: 3.96 (s, 3H, -COOCH₃), 4.50 (s, 2H, 4-SO₂NH₂-C₆H₄-NH-), 7.13 (d, 2H, *J* = 8 Hz, Ar-2',6'-H), 7.35 (t, 2H, *J* = 8 Hz, Ar-3',5'-H), 7.50 (t, 1H, *J* = 7.6 Hz, Ar-4'-H), 7.58 (d, 2H, *J* = 8 Hz, Ar-2,6-H), 7.83 (d, 2H, *J* = 8 Hz, Ar-3,5-H), 8.26 (s, 1H, C-2 proton of pyrimidine), 10.05 (s, 1H, -NH-C₆H₅), 10.31 (s, 1H, 4-SO₂NH₂-C₆H₄-NH-). ¹³C NMR (400 MHz, DMSO-*d*₆) δ PPM: 87.16, 121.65, 122.70, 124.05, 126.36, 128.53, 130.43 (2C), 138.48 (2C), 140.90, 141.73, 149.20 (2C), 158.80 (2C), 159, 167.49. Elemental analysis: Anal. Calcd for C₁₈H₁₇N₅O₄S: C,

54.13; H, 4.28; N, 17.67; O, 16.09; S, 8.05. Found: C, 54.17; H, 4.24; N, 17.70; O, 16.13; S, 8.01. MS (EI) m/z for $C_{18}H_{17}N_5O_4S$, found 400.1 MH^+ .

7.10 Synthesis of methyl-4-(piperazin-1-yl)-6-(phenylamino)pyrimidine-5-carboxylate (6b):

Same as compound **6a**; instead of sulphanilamide, piperazine (0.86g, 0.01mol) was used and refluxed for 2hr yielding white colour solid product of **6b**. (yield 55%, m.p. 164-167°C). 1H NMR (400 MHz, $DMSO-d_6$) δ PPM: 2.14 (s, 1H, -NH- of piperazine), 2.45 (t, 2H, 2,6-position protons of piperazine), 2.58 (t, 2H, 3,5- position protons of piperazine), 3.68 (s, 3H, -COOCH₃), 6.93 (d, 2H, $J = 8$ Hz, Ar-2',6'-H), 7.09 (t, 2H, $J = 8$ Hz, Ar-3',5'-H), 7.42 (t, 1H, $J = 7.6$ Hz, Ar-4'-H), 8.15 (s, 1H, C-2 proton of pyrimidine), 10.16 (s, 1H, -NH-C₆H₅). ^{13}C NMR (400 MHz, $DMSO-d_6$) δ PPM: 51.68 (2C), 55.17 (2C), 87.16, 113.83, 122.68, 124.51, 128.15 (2C), 129.94 (2C), 131.40, 156.08, 160.17, 167.78. Elemental analysis: Anal. Calcd for $C_{16}H_{19}N_5O_2$: C, 61.34; H, 6.19; N, 22.27; O, 10.22. Found: C, 61.37; H, 6.14; N, 22.30; O, 10.25. MS (EI) m/z for $C_{16}H_{19}N_5O_2$, found 314.1 MH^+ .

7.11 Synthesis of methyl-4-(4-methoxyphenylamino)-6-(phenylamino)pyrimidine-5-carboxylate (6c):

Same as compound **6a**; instead of sulphanilamide, 4-methoxyaniline (1.2g, 0.01mol) was used and refluxed for 6hr yielding white colour solid product of **6c**. (yield 95%, m.p. 145-147°C). 1H NMR (400 MHz, $DMSO-d_6$) δ PPM: 3.86 (s, 3H, 4-OCH₃-C₆H₄-NH-), 3.96 (s, 3H, -COOCH₃), 6.91 (d, 2H, $J = 8$ Hz, Ar-2',6'-H), 7.28 (t, 2H, $J = 8$ Hz Ar-3',5'-H), 7.35 (t, 1H, $J = 8$ Hz, Ar-4'-H), 7.42 (d, 2H, $J = 8$ Hz, Ar-3,5-H), 7.60 (d, 2H, $J = 8$ Hz, Ar-2,6-H), 8.15 (s, 1H, C-2 proton of pyrimidine), 9.92 (s, 1H, -NH-C₆H₅), 10.16 (s, 1H, 4-OCH₃-C₆H₄-NH-). ^{13}C NMR (400 MHz, $DMSO-d_6$) δ PPM: 16.47, 76.28, 85.80, 113.63, 117.63, 122.66, 123.78, 124.96 (2C), 126.51 (2C), 128.15, 131.40 (2C), 138.36 (2C), 156.08, 158.94, 160.17. Elemental analysis: Anal. Calcd for $C_{19}H_{18}N_4O_3$: C, 65.12; H, 5.19; N, 15.90; O, 13.2. Found C, 65.17; H, 5.15; N, 15.93; O, 13.7. MS (EI) m/z for $C_{19}H_{18}N_4O_3$, found 351.1 MH^+ .

7.12 Synthesis of methyl-4-(4-nitrophenylamino)-6-(phenylamino)pyrimidine-5-carboxylate (6d): Same as compound (6a); instead of sulphanilamide, 4-nitroaniline (1.4g, 0.01mol) was used and refluxed for 6hr yielding yellow colour solid product of **6d**. (yield 95%, m.p. 160-162°C). ¹H NMR (400 MHz, DMSO-*d*₆) δ PPM: 3.67 (s, 3H, -COOCH₃), 6.14 (d, 2H, *J* = 8 Hz, Ar-2',6'-H), 6.95 (t, 2H, *J* = 8 Hz, Ar-3',5'-H), 6.96 (t, 1H, *J* = 8 Hz, Ar-4'-H), 7.51 (d, 2H, *J* = 8 Hz, Ar-2,6-H), 7.65 (d, 2H, *J* = 8 Hz, Ar-3,5-H), 8.19 (s, 1H, C-2 proton of pyrimidine), 10.03 (s, 1H, -NH-C₆H₅), 10.09 (s, 1H, 4-NO₂-C₆H₄-NH-). ¹³C NMR (400 MHz, DMSO-*d*₆) δ PPM: 14.10, 62.35, 76.23, 125.36, 128.52 (2C), 130.11 (2C), 130.81, 134.22 (2C), 136.31 (2C), 136.35, 137.10, 149.10, 155.85, 169.85. Elemental analysis: Anal. Calcd for C₁₈H₁₅N₅O₄: C, 59.19; H, 4.17; N, 19.16; O, 17.2. Found: C, 59.16; H, 4.15; N, 19.20; O, 17.4. MS (EI) *m/z* for C₁₈H₁₅N₅O₄, found 366.3 MH⁺.

7.13 Synthesis of methyl-4-(4-toluidino)-6-(phenylamino)pyrimidine-5-carboxylate (6e): Same as compound (6a); instead of sulphanilamide, 4-methylaniline (1.07g, 0.01mol) was used and refluxed for 6hr yielding white colour solid product of **6e**. (yield 78%, m.p. 195-197°C). ¹H NMR (400 MHz, DMSO-*d*₆) δ PPM: 3.41 (s, 3H, 4-CH₃-C₆H₄-NH-), 3.67 (s, 3H, -COOCH₃), 7.10 (d, 2H, *J* = 8 Hz, Ar-2',6'-H), 7.14 (t, 2H, *J* = 8 Hz, Ar-3',5'-H), 7.27 (t, 1H, *J* = 8 Hz, Ar-4'-H), 7.36 (d, 2H, *J* = 6.6 Hz, Ar-2,6-H), 7.43 (d, 2H, *J* = 8 Hz, Ar-3,5-H), 8.19 (s, 1H, C-2 proton of pyrimidine), 9.06 (s, 1H, -NH-C₆H₅), 9.14 (s, 1H, 4-CH₃-C₆H₄-NH-). ¹³C NMR (400 MHz, DMSO-*d*₆) δ PPM: 20.37, 51.69, 85.69, 117.66, 120.27, 121.70, 122.80 (2C), 123.88 (2C), 126.51, 128.67, 130.92 (2C), 133.02 (2C), 138.40, 160.14, 169.91. Elemental analysis: Anal. Calcd for C₁₉H₁₈N₄O₂: C, 68.19; H, 5.45; N, 16.49; O, 9.71. Found: C, 68.22; H, 5.41; N, 16.46; O, 9.67. MS (EI) *m/z* for C₁₉H₁₈N₄O₂, found 334 MH⁺.

7.14 Synthesis of methyl-4-ureido-6-(phenylamino)pyrimidine-5-carboxylate (6f): Same as compound (6a); instead of sulphanilamide, urea (0.6g, 0.01mol) was used and refluxed for 2hr yielding white colour solid product of **6f**. (yield 98%, m.p. 200-202°C). ¹H NMR (400

MHz, DMSO- d_6) δ PPM: 3.67 (s, 3H, -COOCH₃), 7.11 (s, 2H, -NH-CO-NH₂), 7.27 (t, 2H, J = 8 Hz, Ar-3',5'-H), 7.36 (d, 2H, J = 8 Hz, Ar-2',6'-H), 7.41 (t, 1H, J = 8 Hz, Ar-4'-H), 7.61 (s, 1H, -NH-C₆H₅), 8.09 (s, 1H, C-2 proton of pyrimidine), 8.22 (s, 1H, -NH-CO-NH₂). ¹³C NMR (400 MHz, DMSO- d_6) δ PPM: 51.43, 76.19, 117.68, 123.30, 126.49 (2C), 128.68 (2C), 129.25, 138.46, 152.19, 165.84, 169.12. Elemental analysis: Anal. Calcd for C₁₃H₁₃N₅O₃: C, 54.17; H, 4.32; N, 24.27; O, 16.28. Found: C, 54.20; H, 4.34; N, 24.30; O, 16.25. MS (EI) m/z for C₁₃H₁₃N₅O₃, found 288.2 MH⁺.

7.15 Synthesis of methyl-4-thioureido-6-(phenylamino)pyrimidine-5-carboxylate (6g):

Same as compound (6a); instead of sulphanilamide, thiourea (0.76g, 0.01mol) was used and refluxed for 2hr yielding white colour solid product of 6g. (yield 75.34%, m.p. 214-216°C). ¹H NMR (400 MHz, DMSO- d_6) δ PPM: 3.26 (s, 3H, -COOCH₃), 6.46 (s, 2H, -NH-CS-NH₂), 7.10 (d, 2H, J = 8 Hz, Ar-2',6'-H), 7.88 (t, 2H, J = 8 Hz, Ar-3',5'-H), 8.18 (t, 1H, J = 8 Hz, Ar-4'-H), 8.31 (s, 1H, -NH-C₆H₅), 8.37 (s, 1H, C-2 proton of pyrimidine), 9.05 (s, 1H, -NH-CS-NH₂). ¹³C NMR (400 MHz, DMSO- d_6) δ PPM: 75.30, 113.10, 115.56, 119.10, 120.81, 125.10 (2C), 129.15 (2C), 133.16, 161.10, 163.14, 170.07. Elemental analysis: Anal. Calcd for C₁₃H₁₃N₅O₂S: C, 51.35; H, 4.33; N, 23.03; O, 10.49; S, 10.59. Found: C, 51.32 H, 4.30, N, 23.08, O, 10.45 S, 10.56 MS (EI) m/z for C₁₃H₁₃N₅O₂S, found 304.4 MH⁺.

7.16 Synthesis of ethyl-4-benzenesulfonamide-6-(phenylamino)pyrimidine-5-carboxylate (6h):

Ethyl-4-chloro-6-(phenylamino)pyrimidine-5-carboxylate (5b) (2.7g, 0.01mol) was mixed with the sulphanilamide (1.72g, 0.01mol) in 15mL of isopropyl alcohol. Catalytic amount of the concentrated HCl was added to the reaction mixture and was refluxed for 6hr and transferred to the crushed ice. White solid of 6h got precipitated out, filtered and dried. (yield 49%, m.p. 214-218°C). ¹H NMR (400 MHz, DMSO- d_6) δ PPM: 1.20 (t, 3H, J = 6.79 Hz, -COOCH₂CH₃), 3.40 (s, 2H, 4-SO₂NH₂-C₆H₄-NH-), 4.13 (q, 2H, J = 6.8 Hz, -COOCH₂CH₃), 7.12 (d, 2H, J = 6.99 Hz, Ar-2',6'-H), 7.33 (t, 2H, J = 6.99 Hz, Ar-3',5'-H),

7.61 (t, 1H, $J = 8$ Hz Ar-4'-H), 7.81 (d, 2H, $J = 9.33$ Hz, Ar-2,6-H), 7.84 (d, 2H, $J = 8$ Hz Ar-3,5-H), 8.31 (s, 1H, C-2 proton of pyrimidine), 10.07 (s, 1H, -NH-C₆H₅), 10.32 (s, 1H, 4-SO₂NH₂-C₆H₄-NH-). ¹³C NMR (400 MHz, DMSO-*d*₆) δ PPM: 13.88, 62.11, 87.36, 121.20, 122.20, 123.91, 126.46 (2C), 128.62 (2C), 129.23, 138.37, 138.43 (2C), 141.71 (2C), 158.81, 159.72, 166.98. Elemental analysis: Anal. Calcd for C₁₉H₁₉N₅O₄S: C, 55.29; H, 4.47; N, 16.39; O, 15.54; S, 7.59. Found: C, 55.25; H, 4.43; N, 16.35; O, 15.57; S, 7.56. MS (EI) m/z for C₁₉H₁₉N₅O₄S, found 414.2 MH⁺. X-crystallographic structure of this compound is shown in (Figure 2).

7.17 Synthesis of ethyl-4-(piperazin-1-yl)-6-(phenylamino)pyrimidine-5-carboxylate (6i):

Same as compound **6h**; instead of sulphanilamide, piperazine (0.86g, 0.01mol) was used and refluxed for 2hr yielding white colour solid product of **6i**. (yield 49.2%, m.p. 179-182°C). ¹H NMR (400 MHz, DMSO-*d*₆) δ PPM: 1.30 (t, $J = 6.8$ Hz, 3H, -COOCH₂CH₃), 2.60 (t, 2H, $J = 8$ Hz, 2,6-position protons of piperazine), 2.65 (t, 2H, $J = 8$ Hz, 3,5-position protons of piperazine), 3.35 (s, 1H, -NH- of piperazine), 4.25 (q, 2H, $J = 6.8$ Hz, -COOCH₂CH₃), 6.40 (d, 2H, $J = 8$ Hz, Ar-2',6'-H), 7.29 (t, 2H, $J = 8$ Hz, Ar-3',5'-H), 7.35 (t, 1H, $J = 8$ Hz, Ar-4'-H), 8.27 (s, 1H, C-2 proton of pyrimidine), 8.32 (s, 1H, -NH-C₆H₅). ¹³C NMR (400 MHz, DMSO-*d*₆) δ PPM: 14.11, 45.91 (2C), 52.85 (2C), 60.78, 115.25, 117.37, 118.25 119.33 (2C), 120.34 (2C), 129.33, 154.22, 166.46, 169.30. Elemental analysis: Anal. Calcd for C₁₇H₂₁N₅O₂: C, 62.16 H, 6.34, N, 21.39, O, 9.47. Found: C, 62.20; H, 6.37; N, 21.36; O, 9.50. MS (EI) m/z for C₁₇H₂₁N₅O₂ found 328.12 MH⁺.

7.18 Synthesis of ethyl-4-(4-methoxyphenylamino)-6-(phenylamino)pyrimidine-5-carboxylate (6j):

Same as compound **6h**; instead of sulphanilamide, 4-methoxyaniline (1.2g, 0.01mol) was used and refluxed for 6hr yielding white colour solid product of **6j**. (yield 78%, m.p. 185-187°C). ¹H NMR (400 MHz, DMSO-*d*₆) δ PPM: 1.41 (t, 3H, $J = 6.8$ Hz, -

COOCH₂CH₃), 3.75 (s, 3H, 4-OCH₃-C₆H₄-NH-), 4.42 (q, 2H, J = 6.8 Hz, -COOCH₂CH₃), 6.92 (d, 2H, J = 8 Hz, Ar-2',6'-H), 7.09 (t, 2H, J = 8 Hz, Ar-3',5'-H), 7.33 (t, 1H, J = 7.6 Hz, Ar-4'-H), 7.46 (d, 2H, J = 8 Hz, Ar-3,5-H), 7.62 (d, 2H, J = 8 Hz, Ar-2,6-H), 8.19 (s, 1H, C-2 proton of pyrimidine), 9.95 (s, 1H, -NH-C₆H₅), 10.13 (s, 1H, 4-OCH₃-C₆H₄-NH-). ¹³C NMR (400 MHz, DMSO-*d*₆) δ PPM: 13.97, 55.18, 60.41, 85.92, 113.72, 122.17, 123.67, 124.00, 124.41 (2C), 128.60 (2C), 129.25, 131.39 (2C), 138.65 (2C), 155.95, 160.02, 167.22. Elemental analysis: Anal. Calcd for C₂₀H₂₀N₄O₃: C, 65.85; H, 5.39; N, 15.47; O, 13.2. Found, C, 65.82; H, 5.37; N 15.43; O, 13.5. MS (EI) m/z for C₂₀H₂₀N₄O₃, found 365.2 MH⁺.

7.19 Synthesis of ethyl-4-(4-nitrophenylamino)-6-(phenylamino) pyrimidine-5-carboxylate (6k): Same as compound **6h**; instead of sulphanilamide, 4-nitroaniline (1.38g, 0.01mol) was used and refluxed for 6hr yielding yellow colour solid product of **6k**. (yield 74%, m.p. 150-153°C). ¹H NMR (400 MHz, DMSO-*d*₆) δ PPM: 1.21 (t, 3H, J = 6.8Hz, -COOCH₂CH₃), 4.14 (q, J = 6.8 Hz, 2H, -COOCH₂CH₃), 6.62 (d, 2H, J = 8 Hz, Ar-2',6'-H), 6.74 (t, 2H, J = 8 Hz, Ar-3',5'-H), 7.27 (t, 1H, J = 7.6 Hz, Ar-4'-H), 7.35 (d, 2H, J = 8 Hz, Ar-2,6-H), 7.87 (d, 2H, J = 8 Hz, Ar-3,5-H), 8.01 (s, 1H, C-2 proton of pyrimidine), 10.01 (s, 1H, -NH-C₆H₅), 11.07 (s, 1H, 4-NO₂-C₆H₄-NH-). ¹³C NMR (400 MHz, DMSO-*d*₆) δ PPM: 13.18, 121.46, 122.91 (2C), 124.20, 125.30 (2C), 128.62, 130.37 (2C), 136.62, 136.33 (2C), 139.23, 140.70, 149.72, 158.85, 159.34, 169.95. Elemental analysis: Anal. Calcd for C₁₉H₁₇N₅O₄: C, 60.3; H, 4.64; N, 18.4; O, 16.89. Found: C, 60.8; H, 4.67; N, 18.36; O, 16.85. MS (EI) m/z for C₁₉H₁₇N₅O₄, found 380.3 MH⁺.

7.20 Synthesis of ethyl-4-(4-toluidino)-6-(phenylamino) pyrimidine-5-carboxylate (6l):

Same as compound **6h**; instead of sulphanilamide, 4-toluidine (1.07g, 0.01mol) was used and refluxed for 6hr yielding white colour solid product of **6l**. (yield 60%, m.p. 205-208 °C). ¹H NMR (400 MHz, DMSO-*d*₆) δ PPM: 1.29 (t, 3H, J = 6.8 Hz, -COOCH₂CH₃), 2.29 (s, 3H, 4-

CH₃-C₆H₄-NH-), 3.45 (q, J = 6.8 Hz, 2H, -COOCH₂CH₃), 6.14 (d, 2H, J = 8 Hz, Ar-2',6'-H), 6.95 (t, 2H, J = 8 Hz, Ar-3',5'-H), 7.10 (t, J = 7.6 Hz, 1H, Ar-4'-H), 7.14 (d, J = 8 Hz, 2H, Ar-2,6-H), 7.29 (d, 2H, J = 8 Hz, Ar-3,5-H), 9.15 (s, 1H, C-2 proton of pyrimidine), 10.03 (s, 1H, -NH-C₆H₅), 10.10 (s, 1H, 4-CH₃-C₆H₄-NH-). ¹³C NMR (400 MHz, DMSO-*d*₆) δ PPM: 12.17, 64.12, 78.31, 120.36, 126.52, 129.81 (2C), 132.11, 134.35 (2C), 135.10 (2C), 137.22, 139.31 (2C), 141.61, 144.10, 146.62, 156.85, 170.85. Elemental analysis: Anal. Calcd for C₂₀H₂₀N₄O₂: C, 68.6; H, 5.67; N, 16.03; O, 9.12. Found: C, 68.57; H, 5.70; N, 16.05; O, 9.15. MS (EI) m/z for C₂₀H₂₀N₄O₂, found 349.2 MH⁺.

7.21 Synthesis of ethyl-4-ureido-6-(phenylamino)pyrimidine-5-carboxylate (6m):

Same as compound **6h**; instead of sulphanilamide, urea (0.67g, 0.01mol) was used and refluxed for 2hr yielding white colour solid product of **6m**. (yield 60.72%, m.p. 215-217°C). ¹H NMR (400 MHz, DMSO-*d*₆) δ PPM: 1.21 (t, 3H, J = 6.8 Hz, -COOCH₂CH₃), 4.10 (q, 2H, J = 6.8 Hz, -COOCH₂CH₃), 6.38 (s, 2H, -NH-CO-NH₂), 7.07 (t, 2H, J = 8 Hz, Ar-3',5'-H), 7.15 (d, 2H, J = 8 Hz, Ar-2',6'-H), 7.50 (s, 1H, -NH-C₆H₅), 7.27 (t, 1H, J = 7.6 Hz, Ar-4'-H), 8.24 (s, 1H, C-2 proton of pyrimidine), 8.41 (s, 1H, -NH-CO-NH₂). ¹³C NMR (400 MHz, DMSO-*d*₆) δ PPM: 14.10, 60.10, 93.20, 113.10, 115.56, 116.41, 118.10 (2C), 129.15 (2C), 145.46, 156.21, 159.23, 168.12. Elemental analysis: Anal. Calcd for: C₁₄H₁₅N₅O₃, C, 55.57; H, 5.30; N, 23.20; O, 15.47. Found: C, 55.60; H, 5.27; N, 23.23; O, 15.50. MS (EI) m/z for C₁₄H₁₅N₅O₃, found 302.2 MH⁺.

7.22 Synthesis of ethyl-4-thioureido-6-(phenylamino)pyrimidine-5-carboxylate (6n):

Same as compound **6h**; instead of sulphanilamide, thiourea (0.76g, 0.01mol) was used and refluxed for 2hr yielding white colour solid product of **6n**. (yield 80.14%, m.p. 219-221 °C).

^1H NMR (400 MHz, $\text{DMSO-}d_6$) δ PPM: 1.24 (t, 3H, $J = 6.8$ Hz, $-\text{COOCH}_2\text{CH}_3$), 4.20 (q, $J = 6.8$ Hz, 2H, $-\text{COOCH}_2\text{CH}_3$), 6.94 (d, 2H, $J = 8$ Hz, Ar-2',6'-H), 7.07 (t, 2H, $J = 8$ Hz, Ar-3',5'-H), 7.84 (t, 1H, $J = 7.6$ Hz, Ar-4'-H), 8.38 (s, 2H, $-\text{NH-CS-NH}_2$), 8.47 (s, 1H, C-2 proton of pyrimidine), 8.61 (s, 1H, $-\text{NH-C}_6\text{H}_5$), 9.01 (s, 1H, $-\text{NH-CS-NH}_2$). ^{13}C NMR (400 MHz, $\text{DMSO-}d_6$) δ PPM: 10.10, 75.10, 115.66, 120.30, 121.81, 125.10, 129.25 (2C), 130.41 (2C), 134.46, 162.10, 164.84, 170.12. Elemental analysis: Anal. Calcd for $\text{C}_{14}\text{H}_{15}\text{N}_5\text{O}_2\text{S}$: C, 52.4; H, 4.73; N, 22.09; O, 10.08; S, 10.3. Found: C, 52.43; H, 4.77; N, 22.04; O, 10.05; S, 10.6 MS (EI) m/z for $\text{C}_{14}\text{H}_{15}\text{N}_5\text{O}_2\text{S}$, found 318.4 MH^+ .

7.23 Antiproliferative *in vitro* assay

All synthesized compounds were evaluated for their anticancer activity against A-375 (Melanoma), MCF-7 (Breast), HEP-3B (Hepatoma) and DU-145 (Prostate) cancer cell lines. To evaluate toxic effects of these compounds, they were also screened against non-cancerous cell line, VERO. For culturing of all these cell lines, DMEM supplemented with 5% HBSS, penicillin, streptomycin and amphotericin B were utilised.²⁵ These cell lines were kept in CO_2 incubator which consisted of humidified atmosphere of 5% CO_2 at 37°C with 90% humidity. Stock solutions of all compounds were prepared in 2% DMSO. Different concentrations of these compounds ranging from $100\mu\text{M}$ to 1nM were prepared from the stock solution. Cells were seeded into 96-well plates and incubated for 24hr. After 24hr, different concentrations of compounds were added into 96-well plate and incubated for 24hr. Effect of compounds was determined after 24hr by performing MTT assay. This assay was performed by using (3-(4,5-dimethylthiazol-2-yl)-2,5-diphenyltetrazolium bromide) solution (20ml of 5mg/ml). This solution was added to each well and incubation was continued for additional 3hr resulted into formation of dark blue formazan crystals within the cells. These crystals were solubilised by

DMSO and absorbance was estimated by ELISA plate reader. IC₅₀ values of all these compounds were determined by non-linear regression method by using Graph pad prism 6.

7.24 Induction of skin cancer²⁶⁻²⁸

All experiments were performed in compliance with the relevant laws and institutional guidelines, and experimental protocols carried out in present study were permitted by the Institutional Animal Ethics Committee (IAEC) of Institute of Pharmacy, Nirma University, Ahmedabad, India (vide protocol number: IP/PCHEM/FAC/15-1/022). All experimental methods are in harmony with CPCSEA guidelines, Ministry of Environment and Forests, Government of India.

Male Swiss-albino mice weighing 25-30g were chosen for the study and were maintained under controlled conditions of temperature ($25^{\circ} \pm 2^{\circ}\text{C}$), humidity ($55 \pm 5\%$) and 12hr light-dark cycle. Male Swiss-albino mice were kept for 1 week acclimatization period. Subsequently the mice were treated with depilatory cream to remove the hairs from the skin, from lumbar region to caudal region of their back. After removing the hairs from the skin, mice were kept for 2 days under standard conditions to check whether the mice were in hair cycle or not. Mice with no hair growth were chosen for the study and were grouped accordingly. Skin cancer was induced by Dimethylbenz(a)anthracene (DMBA) and croton oil. 1mg/ml concentration of DMBA solution was prepared by dissolving 50mg of DMBA in 50ml of acetone. 50 μl of the DMBA solution was sprayed directly at caudal region skin of the mice. Application was made two times in a week, while in 1st week, with period of 2 days gap between the successive doses. Total of 100 μl of DMBA solution was sprayed within 3mm³ area on the caudal skin region of the mice. Two weeks from the initiation of DMBA application, 1% croton oil solution was applied twice a week from 3rd week to 16th week. 1% croton oil was prepared by dissolving 1ml of croton oil in 100ml of acetone. During this, the

treatment with synthesised compounds was started from 7th week and continued till 16th week. Compounds were applied twice a week, followed by application of croton oil in disease induced groups with gap of 1 hour between the two applications.

7.25 Measurement of various parameters²⁶⁻²⁸

At the end of 16th week, blood was collected by retro-orbital puncture from each mice and various parameters were evaluated as per procedure provided in supplementary information. After collection of blood samples, one animal each from all groups were killed and caudal region of skin was excised from the mice, stored in 10% v/v neutral buffered formalin for further histopathological study as detailed in supplementary information.

Electronic Supplementary Information:

Detailed information regarding results of computational approaches; Chromatogram and ^1H NMR, ^{13}C NMR and Mass spectra of few representative compounds; Colour figure and detailed description of results of X-ray crystallography studies; Colour figure with photographs of caudal region skin of the mice and histopathological results of skin samples and pharmacological evaluation methods are available in supplementary information as pdf file. Chem-Draw file of Scheme-1 and original “.cif” files of crystal structure and reflection list are also provided in supplementary information. Crystal structure is deposited at the Cambridge Crystallographic Data Centre with deposition number CCDC 1438291.

Acknowledgement:

The authors are thankful to Nirma University, Ahmedabad, India for providing necessary facilities to carry out the research work.

Abbreviations Used:

5-FU, 5-fluorouracil; DMBA, dimethylbenz(a)anthracene; DMEM, dulbecco's modified eagle's medium; HBSS, hank's balanced salt solution; GGT, gamma glutamyl transferase; LDH, lactate dehydrogenase; CRP, C-reactive protein; MDA, malondialdehyde; GSH, reduced glutathione; SOD, superoxide dismutase.

References

1. WHO website. (www.who.int.) assessed on 1 September **2015**.
2. Rao, A. R.; Sindhuja, H. N.; Dharmesh, S. M.; Sankar, K. U.; Sarada, R.; Ravishankar, G. A. Effective Inhibition of Skin Cancer, Tyrosinase, and Antioxidative Properties by Astaxanthin and Astaxanthin Esters from the Green Alga *Haematococcus pluvialis*. *J. Agric. Food Chem.* **2013**, *61*, 3842–3851
3. Aziz, M. H.; Reagan-Shaw, S.; Wu, J.; Longley, B. J.; Ahmad, N. Chemoprevention of skin cancer by grape constituent resveratrol: relevance to human disease? *FASEB J.* **2005**, *19*, 1193–1195.
4. Sporn, M. B.; Suh, N. Chemoprevention of cancer. *Carcinogenesis*. **2000**, *21*, 525-530.
5. Haque, T.; Rahman, K. M.; Thurston, D. E.; Hadgraft, J.; Lane, M. E. Topical therapies for skin cancer and actinic keratosis. *Eur. J. Pharm. Sci.* **2015**, *77*, 279-289
6. Melnikova, V. O.; Ananthaswamy, H. N. Cellular and molecular events leading to the development of skin cancer. *Mutat. Res.* **2005**, *571*, 91-106
7. Ziegler, A.; Jonason, A. S.; Lefell, D. J.; Simonm, J. A.; Sharma, S. W.; Kimmelman, J.; Remington, L.; Jacks, T.; Brash, D. E. Sunburn and p53 in the onset of skin cancer. *Lett. Nat.* **1994**, *372*, 773-776.
8. Ananthaswamy, H. N.; Loughlin, S. M.; Cox, P.; Evans, R. L.; Ulrich, R. L.; Kripke, M. L. Sunlight and skin cancer: Inhibition of p53 mutation in UV irradiated mouse by sunscreen. *Nat. Med.* **1997**, *3*, 510-514.
9. Simoes, M. C. F; Sousa, J. J. S.; Pais, A. A. Skin cancer and new treatment perspectives: a review, *Cancer Lett.* **2015**, <http://dx.doi.org/doi:10.1016/j.canlet.2014.11.001>.
10. Bramson, H. N.; Corona, J.; Davis, S. T.; Dickerson, S. H.; Edelstein, M.; Frye, S. V; Gampe, R. T.; Harris, P. A.; Hassell, A.; Holmes, W. D.; Hunter, R. N.; Lackey, K. E.;

- Lovejoy, B.; Luzzio, M. J.; Montana, V.; Rocque, W. J.; Rusnak, D.; Shewchuk, L.; Veal, J. M.; Walker, D. H.; Kuyper, L. F. Oxindole-Based Inhibitors of Cyclin-Dependent Kinase 2 (CDK2): Design, Synthesis, Enzymatic Activities, and X-ray Crystallographic Analysis. *J. Med. Chem.* **2001**, *2*, 4339-4358.
11. Echalié, A.; Bettayeb, K.; Ferandin, Y.; Lozach, O.; Cle, M.; Valette, A.; Liger, F.; Marquet, B.; Morris, J. C.; Endicott, J.; Joseph, B.; Meijer, L.; The, D.; Bettayeb, B. Meriolins (3-(Pyrimidin-4-yl)-7-azaindoles): Synthesis, Kinase Inhibitory Activity, Cellular Effects, and Structure of a CDK2/Cyclin A/Meriolin Complex. *J. Med. Chem.* **2008**, 737-751.
12. Alzate-Morales, J. H.; Caballero, J.; Jague, A. V.; Nilo, F. D. G. Insights into the Structural Basis of N2 and O6 Substituted Guanine Derivatives as Cyclin-Dependent Kinase 2 (CDK2) Inhibitors: Prediction of the Binding Modes and Potency of the inhibitors by Docking and ONIOM Calculations. *J. Chem. Inf. Model.* **2009**, *49*, 886-899.
13. Marchetti, F.; Sayle, K. L.; Bentley, J.; Clegg, W.; Curtin, N. J.; Endicott, J.; Golding, B. T.; Griffin, R. J.; Haggerty, K.; Harrington, R. W.; Mesguiche, V.; Newell, D. R.; Noble, M. E. M.; Parsons, R. J.; Pratt, D. J.; Wang, L. Z.; Hardcastle, I. Structure-based design of 2-aryl-amino-4-cyclohexylmethoxy-5-nitroso-6-aminopyrimidine inhibitors of cyclin-dependent kinase 2. *Org. Biomol. Chem.* **2007**, *5*, 1577-1585.
14. Effects, C.; Paprska, M. 4-Arylazo-3, 5-diamino-1H-pyrazole CDK Inhibitors: SAR Study, Crystal Structure in Complex with CDK2, Selectivity, and Cellular Effects. *J. Med. Chem.* **2006**, 6500-6509.
15. Mascarenhas, N. M.; Ghoshal, N. An efficient tool for identifying inhibitors based on 3D-QSAR and docking using feature-shape pharmacophore of biologically active conformation: A case study with CDK2/CyclinA. *Eur. J. Med. Chem.* **2008**, *43*, 2807-

2818.

16. Yang, P.; Myint, K. Z.; Tong, Q.; Feng, R.; Cao, H.; Almehizia, A. A.; Alqarni, M. H.; Wang, L.; Bartlow, P.; Gao, Y.; Gertsch, J.; Teramachi, J.; Kurihara, N.; Roodman G. D.; Cheng, T.; Xie X. Lead Discovery, Chemistry Optimization, and Biological Evaluation Studies of Novel Biamide Derivatives as CB2 Receptor Inverse Agonists and Osteoclast Inhibitors. *J. Med. Chem.* **2012**, 55, 9973–9987.
17. Zhaoa, X.; Yuan, M.; Haung, B.; Zhu, L. Ligand-Based Pharmacophore Model of N-Aryl and N-Heteroaryl Piperazine 1A-Adrenoceptors Antagonists using GALAHAD. *J. Mol. Graph. Model.* **2010**, 29, 126–136.
18. Athri, P.; Wenzler, T.; Tidwell, R.; Bakunova, S. M.; Wilson W. D. Pharmacophore Model for Pentamidine Analogs Active Against Plasmodium Falciparum. *Eur. J. Med. Chem.* **2010**, 18, 6147-6151.
19. Cabellero, J. 3D-QSAR (CoMFA and CoMSIA) and Pharmacophore (GALAHAD) Studies on the Differential Inhibition of Aldose by Flavonoid Compounds. *J. Mol. Graph. Model.* **2010**, 435-476.
20. Dong, X.; Zhou, X.; Jing, H.; Chen, J.; Liu, T.; Yang, B.; He, Q.; Hu, Y. Pharmacophore Identification, Virtual Screening, and Biological Evaluation of Prenylated Flavonoids Derivatives as PKB/Akt1 Inhibitors. *Eur. J. Med. Chem.* **2011**, 1023-1066.
21. Bhatt, H.; Pannecouque, P.; Patel, P.; Discovery of HIV-1 Integrase Inhibitors: Pharmacophore Mapping, Virtual Screening, Molecular Docking, *In silico* ADMET Studies. *Chem. Biol. Drug. Des.* **2013**, 1-13.
22. Vyas, V.; Ghate, M.; Goel, A. Pharmacophore Modeling, Virtual Screening, Docking and *In Silico* ADMET Analysis of Protein Kinase B (PKB) Inhibitors. *J. Mol. Graph. Mode.* **2013**, 42, 17–25.

23. Krishna, S.; Singh, D. K.; Meena, S.; Datta, D.; Siddiqi, M. I.; Banerjee, D. Pharmacophore-Based Screening and Identification of Novel Human Ligase I Inhibitors with Potential Anticancer Activity. *J. Chem. Inf. Model.* **2014**, *54*, 781.
24. Chhabria, M. T.; Bhatt, H. G.; Raval, H. G.; Oza, P. M. Synthesis and biological evaluation of some 5-ethoxycarbonyl-6-isopropylamino-4-(substitutedphenyl) aminopyrimidines as potent analgesic and anti-inflammatory agents. *Bioorg. Med. Chem. Lett.* **2007**, *17*, 1022-1024.
25. Vyas, V. K.; Variya, B.; Ghate, M. D. Design, synthesis and pharmacological evaluation of novel substituted quinoline-2-carboxamide derivatives as human dihydroorotate dehydrogenase (hDHODH) inhibitors and anticancer agents. *Eur. J. Med. Chem.* **2014**, *82*, 385-393.
26. Hsu, C. H.; Ho, Y. S.; Lai, C. S.; Hsieh, S. C.; Chen, L. H.; Lin, E.; Ho, C. T.; Pan M. H; Hexahydro- β -Acids Potently Inhibit 12-O-Tetradecanoylphorbol 13-Acetate-Induced Skin Inflammation and Tumor Promotion in Mice. *J. Agric. Food Chem.* **2013**, *61*, 11541–11549.
27. Chen, H. M.; Lee, Y. H.; Wang, Y. J. ROS-Triggered Signaling Pathways Involved in the Cytotoxicity and Tumor Promotion Effects of Pentachlorophenol and Tetrachlorohydroquinone. *Chem. Res. Toxicol.* **2014**, DOI: 10.1021/tx500487w.
28. Subramanian, V.; Venkatesan, B.; Tumala, A.; Vellaichamy, E. Topical application of Gallic acid suppresses the 7,12-DMBA/Croton oil induced two-step skin carcinogenesis by modulating anti-oxidants and MMP-2/MMP-9 in Swiss albino mice. *Food. Chem. Toxicol.* **2014**, *66*, 44-55.

Figure Captions

Scheme 1. Reagents and conditions: (i) Aq. KOH, DMF, stirring with cooling for 10min; (ii) Carbon disulphide, stirring at 25°C for 1hr; (iii) Dimethyl sulphate, stirring at 0°C; (iv) Aniline, Ethanol, reflux for 2hr; (v) Formamidine acetate in ethanolic NaOH, stirring at 0-5°C for 6hr; (vi) 1,4-dioxane saturated with HCl, stirring for 24hr; (vii) Aromatic / aliphatic amines, IPA, few drops of concentrated HCl, reflux for 2-6hr.

Figure 1. 2D representation of best pharmacophore model generated through GALAHAD module of Sybyl X.

Figure 2. Determination of structure of the compound **6h** by X-ray crystallographic studies.

Figure 3. Measurement of serum biomarkers after the treatment with 5-FU and compounds **6a**, **6h**, **6j** and **6k**, where each bar represents Mean \pm SEM, n = 6 mice (Oneway ANOVA followed by Dunnett's multiple comparison test), * = p < 0.05 vs normal control group: (A) Gamma glutamyl transferase level; (B) Lactate dehydrogenase level; (C) C-reactive protein level.

Figure 4. Measurement of oxidative stress parameters after the treatment with 5-FU and compounds **6a**, **6h**, **6j** and **6k**, where each bar represents Mean \pm SEM, n = 6 mice (Oneway ANOVA followed by Dunnett's multiple comparison test), * = p < 0.05 vs normal control group: (A) Malondialdehyde level; (B) Glutathione level; (C) Super oxide dismutase level.

Figure 5. Comparison of the growth of tumour volume and tumour burden of normal control group and skin cancer control group with significant reduction in groups of animals treated with 5-FU, compounds **6a**, **6h**, **6j** and **6k**: (A) Tumour volume; (B) Tumour burden.

Figure 6. Photographs of caudal region skin of the mice and histopathological results of skin samples: (A) Normal control group; (B) Skin cancer control group; (C) Skin cancer treated with 5-FU; (D) Skin cancer treated with compound **6h**.

TABLE 1. *In-vitro* antiproliferative activity of 5-FU and synthesized compounds on various cancer cell lines.

Compounds	A-375	MCF-7	HEP-3B	DU-145	VERO
	IC ₅₀ (μM)	IC ₅₀ (μM)	IC ₅₀ (μM)	IC ₅₀ (μM)	IC ₅₀ (μM)
5-FU	0.0042	1.60	1.75	0.07	>500
SERIES-1					
6a	0.0073	0.0101	2.5188	>100	>500
6b	0.1576	3.1948	0.239	0.0073	>500
6c	0.1443	0.0659	2.8571	>100	0.007
6d	0.4960	2.6525	>100	0.11	0.03
6e	1.5750	1.9007	3.0120	3.01	0.002
6f	0.6538	0.0548	3.4843	>100	>500
6g	5.615	0.0541	0.2240	>100	>500
SERIES-2					
6h	0.0047	0.0075	0.0222	0.0075	>500
6i	3.058	3.058	0.0386	>100	0.0121
6j	0.0079	0.0042	2.7472	2.7472	>500
6k	0.0876	0.0120	0.0561	25.8877	>500
6l	0.258	2.8735	0.018	2.8735	0.055
6m	0.95	3.8461	0.0302	3.6339	>500
6n	1.21	0.016	3.8314	0.9745	>500

TABLE 2. Effect of 5-Fluorouracil (2%) and compounds 6a, 6h, 6j, and 6k (2%) on serum levels of Gamma glutamyl transferase (GGT), Lactate dehydrogenase (LDH), C-reactive protein (CRP)

Parameters	CON	COF	SCF	6a	6h	6j	6k
GGT	6.17 ±	39.53 ±	8.68 ±	12.66 ±	11.19 ±	25.16 ±	25.12 ±
(unit/L)	0.92	0.82	0.57	0.43	0.98	0.97	1.98
LDH	170.6 ±	790.1 ±	191.7 ±	753.3 ±	262.7 ±	355.2 ±	378.7 ±
(unit/L)	0.21	1.53	0.56	1.91	0.58	0.62	0.64
CRP	3.86 ±	28.44 ±	4.42 ±	7.66 ±	5.75 ±	24.14 ±	7.00 ±
(mg/dl)	0.28	1.19	0.22	0.25	0.27	1.67	0.20

Each column represents Mean ± SEM, n = 6 mice (Oneway ANOVA followed by Dunnett’s multiple comparison test); GGT: Gamma glutamyl transferase; LDH: Lactate dehydrogenase; CRP: C-reactive protein; CON: Normal control group; COF: Skin cancer control group; SCF: Skin cancer control group treated with 5-FU.

TABLE 3. Effect of 5-Fluorouracil (2%) and compounds 6a, 6h, 6j, and 6k (2%) on serum levels of Malondialdehyde (MDA), Reduced glutathione (GSH) and Superoxide dismutase (SOD) levels.

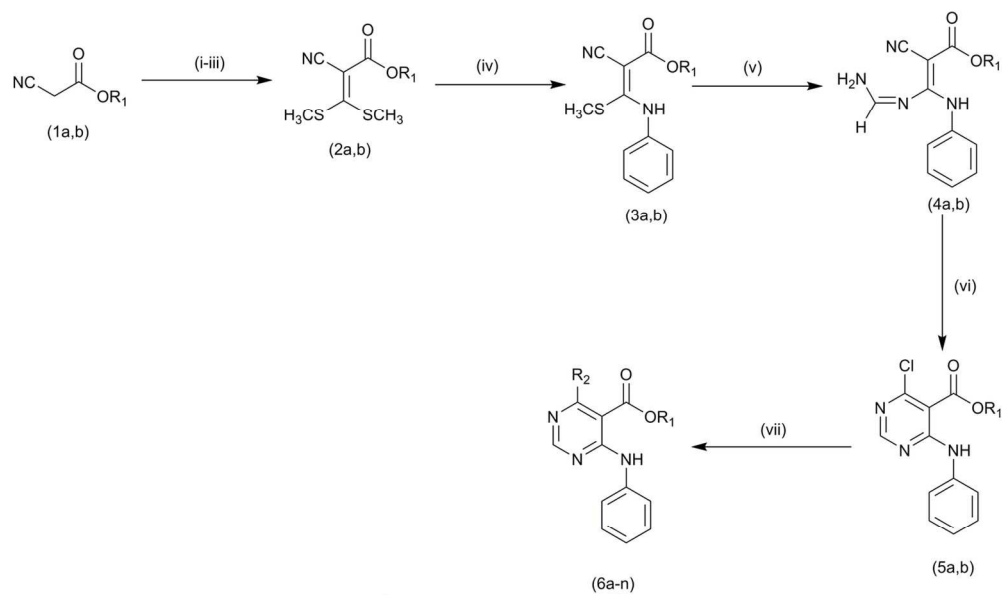
Parameters	CON	COF	SCF	6a	6h	6j	6k
MDA	38.46 ±	95.30 ±	53.42 ±	78.21 ±	68.38 ±	89.74 ±	75.80 ±
(nmol/mg)	0.31	0.35	0.37	0.36	0.37	0.32	0.39
GSH	52.13 ±	18.18 ±	51.32 ±	28.92 ±	51.60 ±	34.82 ±	30.07 ±
(nmol/mg)	0.20	0.19	0.23	0.12	0.10	0.31	0.15
SOD	3.72 ±	2.51 ±	3.59 ±	2.62 ±	3.50 ±	2.62 ±	2.66 ±
(unit/mg)	0.48	0.45	0.43	0.42	0.49	0.42	0.42

Each column represents Mean ± SEM, n = 6 mice (Oneway ANOVA followed by Dunnett's multiple comparison test); MDA: Malondialdehyde; GSH: Reduced glutathione; SOD: Superoxide dismutase; CON: Normal control group; COF: Skin cancer control group; SCF: Skin cancer control group treated with 5-FU.

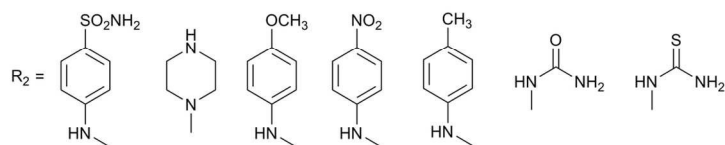
TABLE 4. Effects of 5-Fluorouracil (2%) and compounds 6a, 6h, 6j, and 6k (2%) on Tumour volume, Tumour burden and Survival Rate.

Groups Treated with	Parameters	Number of Weeks					
		6	8	10	12	14	16
CON	Tumour Volume	0	0	0	0	0	0
	Tumour Burden	0	0	0	0	0	0
	Survival Rate	100%	100%	100%	100%	100%	100%
COF	Tumour Volume	1.53	3.12	7.69	15.99	24.30	27.76
	Tumour Burden	6.53	18.12	39.69	87.99	144.30	167.76
	Survival Rate	100%	100%	100%	100%	83.33%	66.66%
SCF	Tumour Volume	1.58	3.15	7.01	4.50	2.10	2.19
	Tumour Burden	6.28	19.15	37.01	16.91	10.10	8.89
	Survival Rate	100%	100%	100%	100%	100%	100%
6a	Tumour Volume	1.46	3.97	7.80	8.14	7.14	6.10
	Tumour Burden	6.46	20.97	40.80	32.54	26.64	24.05
	Survival Rate	100%	100%	100%	83.33%	66.66%	66.66%
6h	Tumour Volume	1.14	3.79	7.91	5.00	4.12	2.95
	Tumour Burden	6.14	18.79	34.91	17.01	15.52	11.32
	Survival Rate	100%	100%	100%	100%	100%	100%
6j	Tumour Volume	1.13	3.16	7.70	6.34	5.11	4.31
	Tumour Burden	6.13	19.16	38.70	24.64	19.61	16.31
	Survival Rate	100%	100%	100%	100%	100%	100%
6k	Tumour Volume	1.104	3.425	7.232	7.882	6.150	5.000
	Tumour Burden	6.804	20.42	40.23	30.68	21.472	16.770
	Survival Rate	100%	100%	100%	66.66%	50%	50%

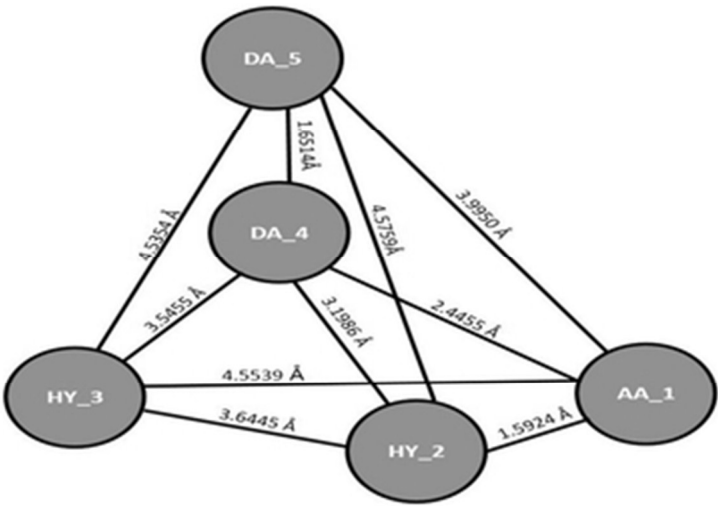
CON: Normal control group; COF: Skin cancer control group; SCF: Skin cancer control group treated with 5-FU.



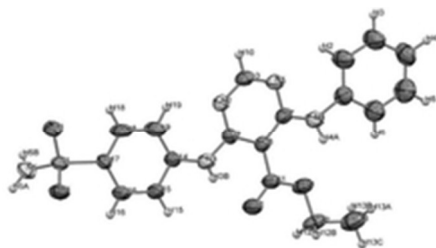
R₁ = (a) -CH₃, (b) -C₂H₅



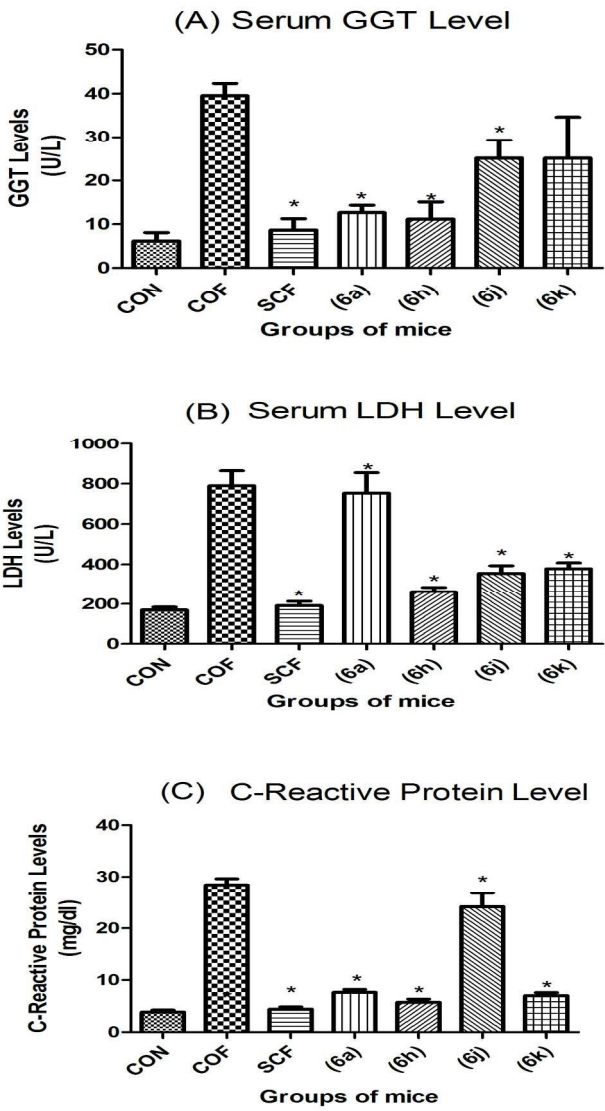
127x105mm (300 x 300 DPI)



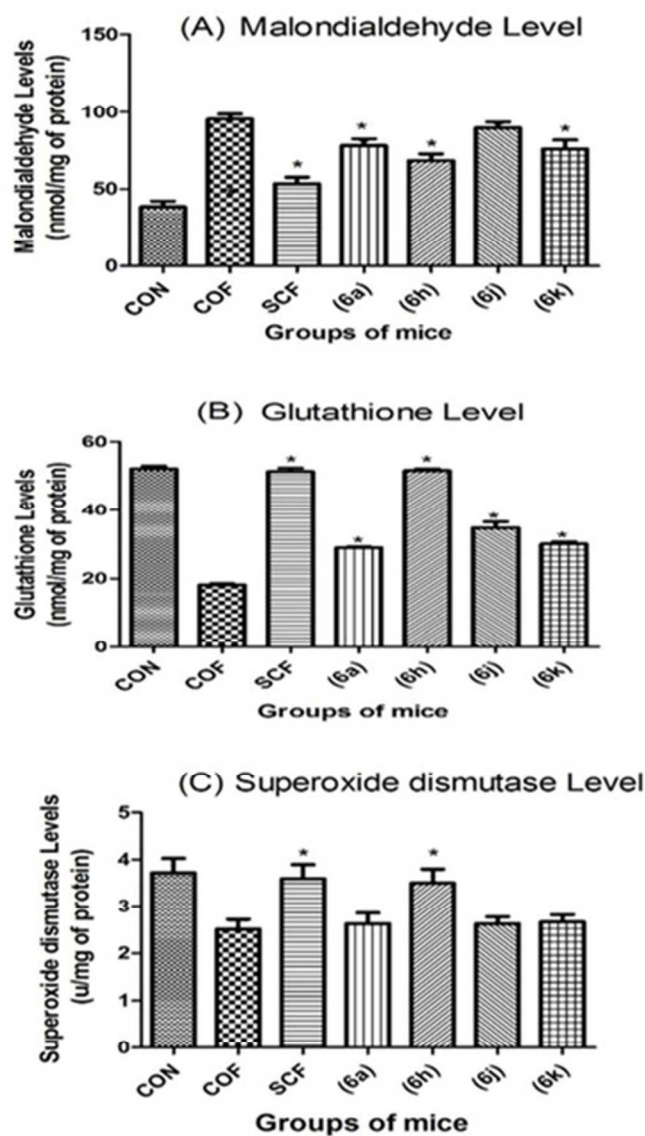
15x10mm (600 x 600 DPI)



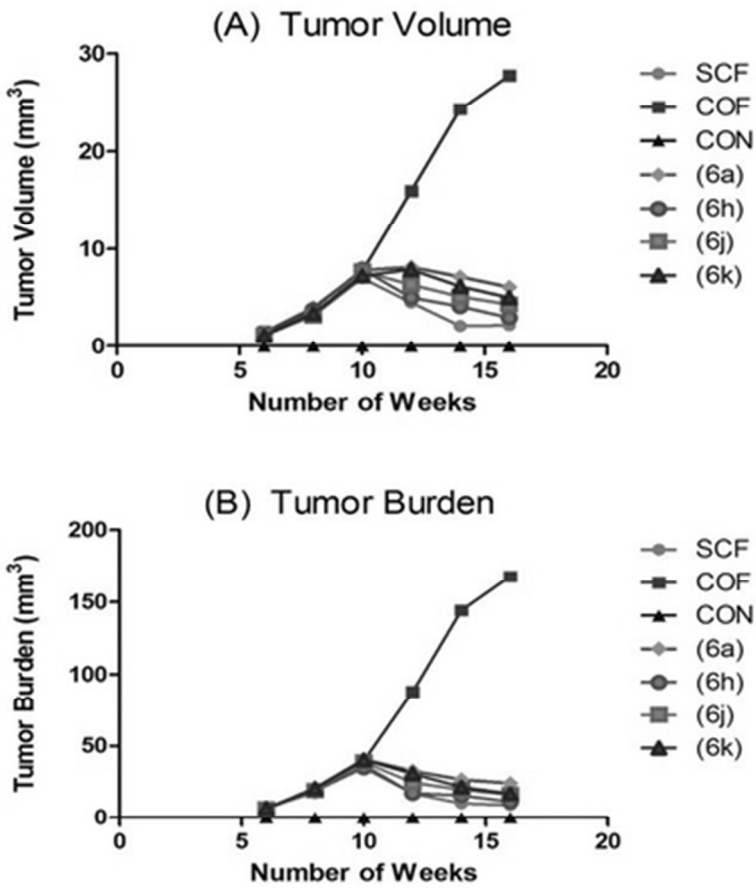
9x5mm (600 x 600 DPI)



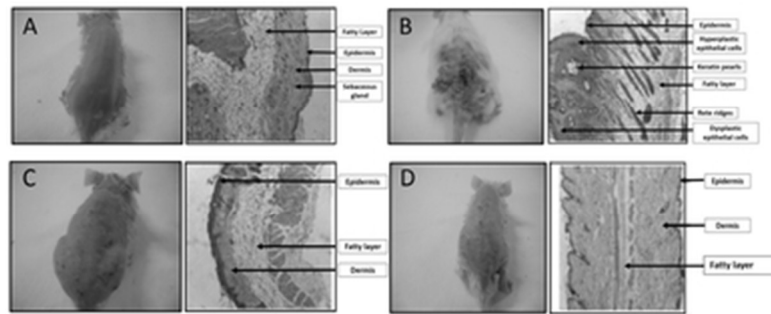
94x176mm (600 x 600 DPI)



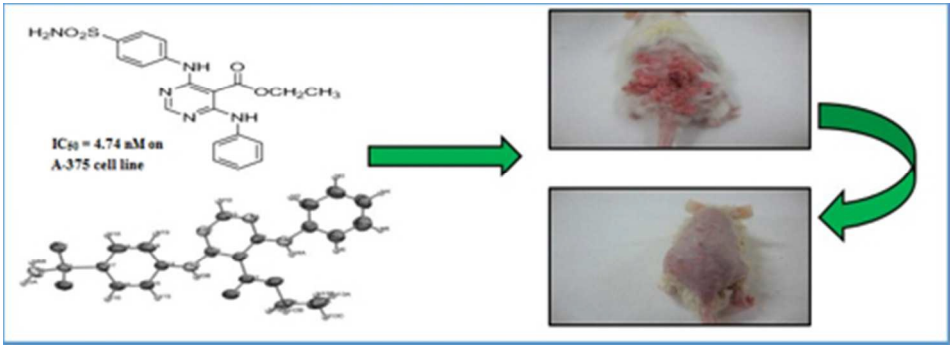
17x28mm (600 x 600 DPI)



16x20mm (600 x 600 DPI)



16x6mm (600 x 600 DPI)



80x28mm (150 x 150 DPI)